Journal of Geochemical Exploration 199 (2019) 16–30

Contents lists available at ScienceDirect

Journal of Geochemical Exploration

journal homepage: www.elsevier.com/locate/gexplo

# Identification of geochemical anomalies of the porphyry–Cu deposits using concentration gradient modelling: A case study, Jebal-Barez area, Iran

Mansour Ziaii[a], Samaneh Safari[a], Timofey Timkin[b,*], Valery Voroshilov[b], Tamara Yakich[b]

[a] Faculty of Mining, Petroleum & Geophysics Engineering, Shahrood University of Technology, Iran
[b] School of Earth Sciences & Engineering, Tomsk Polytechnic University, 634050 Tomsk, Russia

ARTICLE INFO

*Keywords:*
Concentration gradient modelling
Zone dispersed mineralization (ZDM)
Blind mineralization (BM)
Identification of geochemical anomalies (IGA)

ABSTRACT

This paper presents a novel gradient model for exploration of blind mineralization. The concentration gradient coefficient techniques have been proved to be very well-suited for typical mining geochemistry applications. Gradient concentration corresponds to concentration variations. Large concentration changes due to geochemical data distribution correspond to surfacing anomaly, and less concentration variations are more likely to be related to the deeper geochemical anomalies. The introduced technique is capable to distinguish the difference between the blind mineralization and zone dispersed mineralization, computationally and without exploration drilling. In this research, deep geochemical anomalies are investigated using the gradient concentration values for the porphyry–Cu deposits of the Jebal-Barez region in Iran. Based on the results obtained from the proposed gradient model, values > 1.0 in G(Vz) reveal the existence of blind mineralization in the study zone. The findings based on this method suggest that SW of Jebal-Barez is a highly favourable zone for exploration of blind mineralization. The value for G(Vz) in this zone is equal to 5.04. The results obtained in this research were consistent well with the findings of the previous research in the area and the detected Kerver as the main blind mineralization in Jebal-Barez. A local exploration was carried out in this zone in four areas of Kerver using the gradient model.

## 1. Introduction

Concentration gradient (CG) shows the change of elements concentration. There is a big change in the curves or surfaces, in which the gradient is the greatest (Chen et al., 2017). CG is a significant characteristic geological parameter. In general, the traditional methods do not consider CG for exploration of deposits (Cheng et al., 1994, 1996), and various methods have been used for a geochemical anomaly separation (Govett et al., 1975; Solovov and Matveev, 1985; Grigorian and Ziaii, 1997; Cheng, 1999; Li et al., 2003; Afzal et al., 2011; Matveev and Solovov, 2011; Zuo et al., 2013; Mohammadi et al., 2013; Timkin et al., 2014; Cheng et al., 2014; Soltani et al., 2014 and Vorobiev, 2016).

Recognition of the blind and false anomalous patterns is a typical scenario of a complex mining system. In the past, several models have been developed to predict the geochemical anomalies at a mine scale. Most of the models are concerned solely with the identification of geochemical anomalies (IGA). The multivariate anomaly recognition in geochemical exploration is defined here as blind mineralization (BM), outcropping, and zone dispersed mineralization (ZDM).

An important point that should be considered in the interpretation of secondary geochemical haloes is the erosion level of a mineral deposit since it affects the size and extent of anomalies in the soil. This fact has been conceptualized by different examples known as the models (a) blind economic mineralization, (b) outcropping economic mineralization, and (c) dispersed zone mineralization (Beus and Grigorian, 1977; Levinson, 1980; Ovchinnikov and Grigoryan, 1978; Solovov, 1987). Soil anomalies associated with outcropping economic mineralization would be normally stronger than those associated with blind mineralization, and they may be erroneously assumed to be more promising than the others unless the erosion levels are taken into account. Soil anomalies based on the ZDM model may be similar in intensity to those associated with the blind mineralization. However, if they are not properly interpreted, fruitless exploration may be the result. Root zones of some types of ore deposits typically have a different metal association with the ore zone and leakage (upper) zones, and these associations may be helpful in identifying the relationship of a soil anomaly to mineralization. Characterizing horizons of erosional surfaces of a steeply dipping ore body and its primary halo in host rocks is a problem with no direct solution. There are two generally reliable

* Corresponding author.
*E-mail address:* timkin@tpu.ru (T. Timkin).

https://doi.org/10.1016/j.gexplo.2019.01.004
Received 11 January 2018; Received in revised form 9 January 2019; Accepted 15 January 2019
Available online 17 January 2019
0375-6742/ © 2019 Elsevier B.V. All rights reserved.

ways of acquiring knowledge from IGA, including laboratory measurements and vertical zonality coefficient interpretation. Laboratory measurement of the cores obtained from the field or sample archives provide a precise (assuming adequate equipment) vertical zonality coefficient of values (Beus and Grigorian, 1977; Levinson, 1980). These are used in the geochemical simulation studies as well as any other design and development studies in the field. Another method for IGA determination is a geochemical model of mineralization in bedrock and soils (Grigorian, 1985; Harraz and Hamdy, 2015).

In this research, a new geochemical model was introduced for IGA determination. The proposed methodology, which is based on CG, is quite inexpensive compared to the traditional exploration methods. These values are comparable to those obtained by laboratory measurements on core samples. A feasibility study based on the proposed method for the IGA estimation represents the effective and useful results. A research on the CG methods for exploration of ore deposits dates back to 1961, when the first survey of this type was carried out by Sochevanov (Sochevanov, 1961).

This model was presented in the Jebal-Barez region. Previous researches regarding this region have shown that the Kerver area located in SW of Jebal-Barez is favourable for local exploration of blind mineralization (Safari et al., 2016; Ziaii et al., 2011). Borna and Sodishoar (2005) have studied the blind porphyry copper deposits at the Kerver area (Kerver1 and Kever2) using the zonality method in a local scale.

In this study, an exploration of the blind porphyry copper deposit was carried out in a regional scale in Jebal-Barez using CG. Then we focused on the SW of Jebal-Barez that it has high prospectivity for porphyry copper mineralization.

For this purpose, the CG values for the sub-ore and supra-ore elements were mapped, and the G(Vz) values (ratio of the supra-ore gradient to the sub-ore gradient) were calculated in local anomalies of gradient map. Supra ore and sub ore elements form in top and bottom of deposit respectively in the composition of hydrothermal orebody (Beus and Grigorian, 1977). Concentration gradient demonstrate of concentration change and, the very low change of elements is related to the deep geochemical anomalies while the high concentration change is related to surface anomaly. Therefor we expect in blind mineralization, that supra ore elements exist on the surface and sub ore elements are on the depth of earth, concentration change value for supra elements be higher than this value in sub ore elements. Safari et al. (2017) tested this hypothesis for the separation of BM to ZDM for three typical standard ore deposits using data from NW Iran and the Inza area of British Colombia, Canada. Each typical standard ore deposits represented different BM/ZDM and Situate in dissimilar landscapes under different host rock, landscape, alteration and mineralogical, geochemical type (genetic model). They investigated change values using gradient parameter and presented the model for detection of blind mineralizaion base on concentration gradient (Safari et al., 2017; Safari, 2017).

In this paper gradient model was done for exploration of blind mineralization in Jebal Barez.

## 2. Geological setting of studied area

The studied area is located in the Shar-e-Babak–Bam ore field in the southern part of the Central Iranian volcano–plutonic magmatic arc (Fig. 1). This region is a part of the Sahand-Bazman arc belt.

In terms of geology, this region can be divided into two parts with the WN to ES direction. The upper section is a part of the Bam plain that has been covered by a relatively recent sediment and rubble. The lower section is a part of the Jebal-Barez Mountains consisting the volcanic and intrusive rocks. Ranges of the NW–SE trending Kuh-e Jebal-Barez mountain are cut through the studied area form a part of the Sahand–Basman Tertiary volcanic belt and metallogenic province within the Central Iranian volcano plutonic magmatic arc (Borna and Sodishoar, 2005; Bedakhshan and Sodishoar, 2000). This section contains multiple high mountains, while the highest is around 3741 m. In this area, there are several perennial rivers. The volcanic activity in the area started from the Late Cretaceous and continued to the Middle–Late Eocene (Valeh, 1972). Large masses of granite and granodiorite outcrops can be found in the south and ES of the region. In addition to these masses, several dacite domes were formed in the area. These dacite domes cover the volcanoclastic rocks. These zonal patterns exhibit porphyry copper deposit with the first tow subzones being more important (Ghorbani, 2013). In Jebal-Barez Mountains most of copper deposits are typically associated with veins in faulted andesite, granodiorite and diorite are associated with dykes. This area is special importance due to presence of copper mineralization and limited iron, lead and zinc mineralization. Several copper mineral indices have been identified in Jebalbarz include Kerver, Vouved, Rudad, Sartaqin, Gigu, Amjaz, Band-e- Razou, DahanahBizgou, GivMard, Beneh Char, Anarak-e-Bala, Khorou-Darrud. Kerver area introduce as an important in this region (Bedakhshan and Sodishoar, 2000). The regional mapping of the Kerman Cenozoic magmatic arc reveals distinctive patterns of the argillic and phyllicrocks that can be associated with the regional structural features and tectonic processes and that can be used in regional mineral assessments. Most of the known porphyry–Cu deposits in this region are characterized by well-developed zonal patterns of mineralization and hydrothermal alterations. These zonal patterns exhibit significant differences in terms of major oxides and trace element contents reflecting variations in mineralogical and geochemical compositions of the mineralized and hydrothermally altered zones. Alteration of the region has been formed around the semi-deep masses and main fractures. According to the intrusive masses, the trend of alteration zone is from WN to ES. Alterations in the region are Propylitic, Argillic, Silica, Fused Quartz, Potassic, Alunite, and Oxide. Mineralization in the area includes Pyrite, Malachite, Azurite, Chalcopyrite, Bornite, iron oxide (Hematite, Limonite), and manganese oxides (Fig. 1).

## 3. Methodology

Here, individual uni-element data was interpolated in the case studies. Values within the interpolated element maps were individually rescaled to the range of 0, 1 (Ziaii et al., 2011).

The multiplicative geochemical gradient data of sub-ore element (Cu × Ag) and supra-ore elements (Pb × Zn) were created separately for each area.

Jebal-Barez is porphyry copper deposit and the elements Mo, Cu and Ag are sub-ore elements and the elements Pb, Zn and Bi are supra- ore elements in this type of deposits. Ziaii et al. (2009) presented a geochemical model by studying three porphyry copper deposits including Aktogy (Kazakhstan), Asarel (Bulgaria) and Tekhut (Armenia) (See the Fig. 1 in Ziaii et al., 2011). The geological settings of these deposits are different nevertheless this model suggests the existence of a quantitatively uniform vertical geochemical zonality in the structure of primary haloes of the deposits. This model introduces three vertical zonalities including $VZ1 = Pb \times Zn/Cu \times Mo$, $VZ2 = Pb \times Zn/Cu \times Ag$ and $VZ3 = Pb \times Zn \times Bi/Cu \times Ag \times Mo$ for porphyry copper deposits.

The CG calculation was carried out in both the x and y directions using Eqs. (2) and (3) in the Matlab Software package. The spatial distribution patterns for the sub-ore and supra-ore gradients were shown in the geochemical maps. Local anomalies of the sub-ore pathfinder element gradient and supra-ore gradient were recognized in the geochemical maps.

The average CG value was calculated in each local anomaly for the sub-ore and supra-ore gradient maps. Indices of gradient geochemical zonality (G(Vz)) were calculated from ratios of the supra-ore to the sub-ore pathfinder element gradients around the mineral deposits.

On the other hand, vertical zonalities were calculated using areal productivity of elements and the results were compared with obtained results of presented method in this paper.

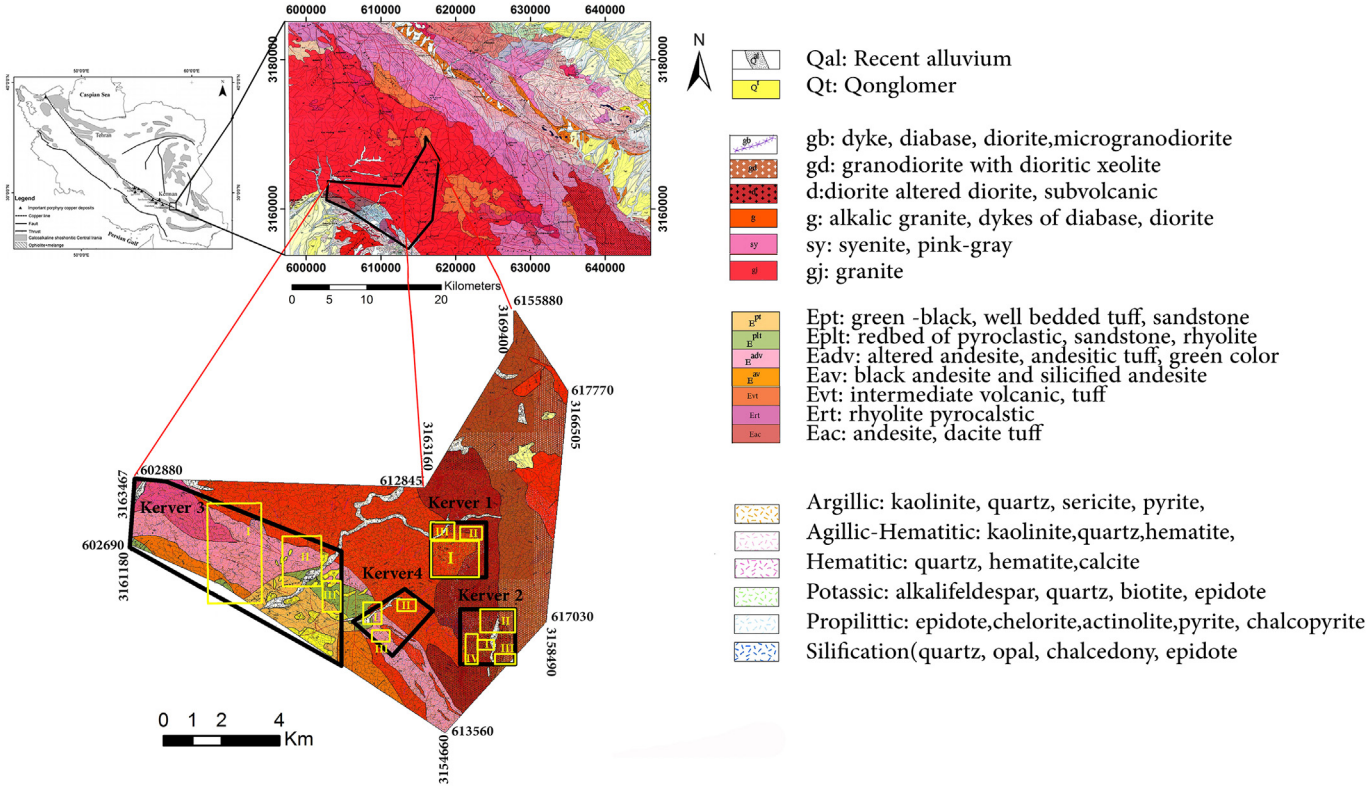


**Fig. 1.** Geological map of Jebal-Barez area.
(Modified from Afaghi et al., 1959; Dorri, 2006).

### 3.1. Properties of geochemical data and geochemical anomalies

In a regional scale, 490 samples of stream sedimentary were taken from Jebal-Barez. This geochemical data subset represents a total drainage basin area. The samples were analyzed for Cu, Zn, Ag, Pb, Au, W, As, Hg, Ba, and Bi by the atomic absorption method.

Totally, 932 samples were taken from four areas consisting of Kerver1, Kerver2, Kerver3 and Kerver4 in a local scale. Additionally, six exploratory drilled boreholes were excavated in the Kerver2 area, and 1253 samples were taken from these boreholes. The samples were submitted to the laboratory for chemical analysis. The concentrations of 22 elements were determined by the Nonferrous Metal Guilin Minerals Geology Testing Center in China. While all samples were analyzed for twenty elements, here we only discuss specific elements, namely Cu, Ag, Pb, and Zn. Locations of the samples in the SW part of the Jebal-Barez area are shown in Figs. 1 and 2.

### 3.2. Concentration gradient (CG) method

Geochemical gradient refers to the content change rate of unit distance, where the ore element is spread out. In addition, there is a rate change between two adjacent elements (Bingli et al., 2013; Ke et al., 2007; Zhou et al., 2012). Initially, Sochevanov (1961) suggested, using as a criterion, the uneven distribution of the element content of the gradient, which can be determined by the difference in element content between each two adjacent samples (Eq. (1)).

$$Gr = |\Delta c|/\Delta x \tag{1}$$

In Eq. (1), Δc is the difference in element concentration in two adjacent samples in ppm, Δx is the distance between two adjacent samples in meters in the x direction, and Gr is the concentration gradient (CG) in ppm/m.

In two dimensions, the gradient is given by the following formula (Gonzalez and Richard, 2002):

$$\nabla f = grad(f) = \begin{bmatrix} g_x \\ g_y \end{bmatrix} = \begin{bmatrix} \partial f/\partial x \\ \partial f/\partial y \end{bmatrix} \tag{2}$$

This vector ($\nabla f$) has an important geometrical property that points in the direction of the greatest rate of change at location (x, y). In Formula (2), $\frac{\partial f}{\partial x}$ is the gradient in the x direction and $\frac{\partial f}{\partial y}$ is the gradient in the y direction.

The magnitude of the vector $\nabla f$ denotes M(x, y), where:

$$M(x,y) = mag(\nabla f) = \sqrt{{g_x}^2 + {g_y}^2} \tag{3}$$

In order to calculate the gradient for each sample, the ratio of difference between adjacent sample and also interval of two samples were determined. Sampling interval was considered as interval of x, y in Eq. (1). Also, the total gradient was calculated by Eq. (3) based on obtaining the gradient in x, y directions.

The CG method can distinguish the sub-ore elements from the supra-ore ones in geochemical haloes. It decreases the effect of the background content in calculating the geochemical anomalies. It introduces a special approach to enhance weak geochemical haloes and to extend their size (Ziaii, 2008).

### 3.3. Areal productivity

The areal productivity is used in the area where multiple samples and anomalies are presented. Average metal content in an orebody and effective surface of geochemical anomalies is the non-parametric index. The numerical value of non-parametric characterize does not illustrate natural properties of the object of study. So, geochemical parameters are invariably preferable to show distribution of the geochemical field. The important parametric meaning for characteristic of geochemical anomalies is provided by the areal productivity which is the most reliable criteria in exploration. This parameter is calculated as the amount of chemical element in excess of the background value, along particular

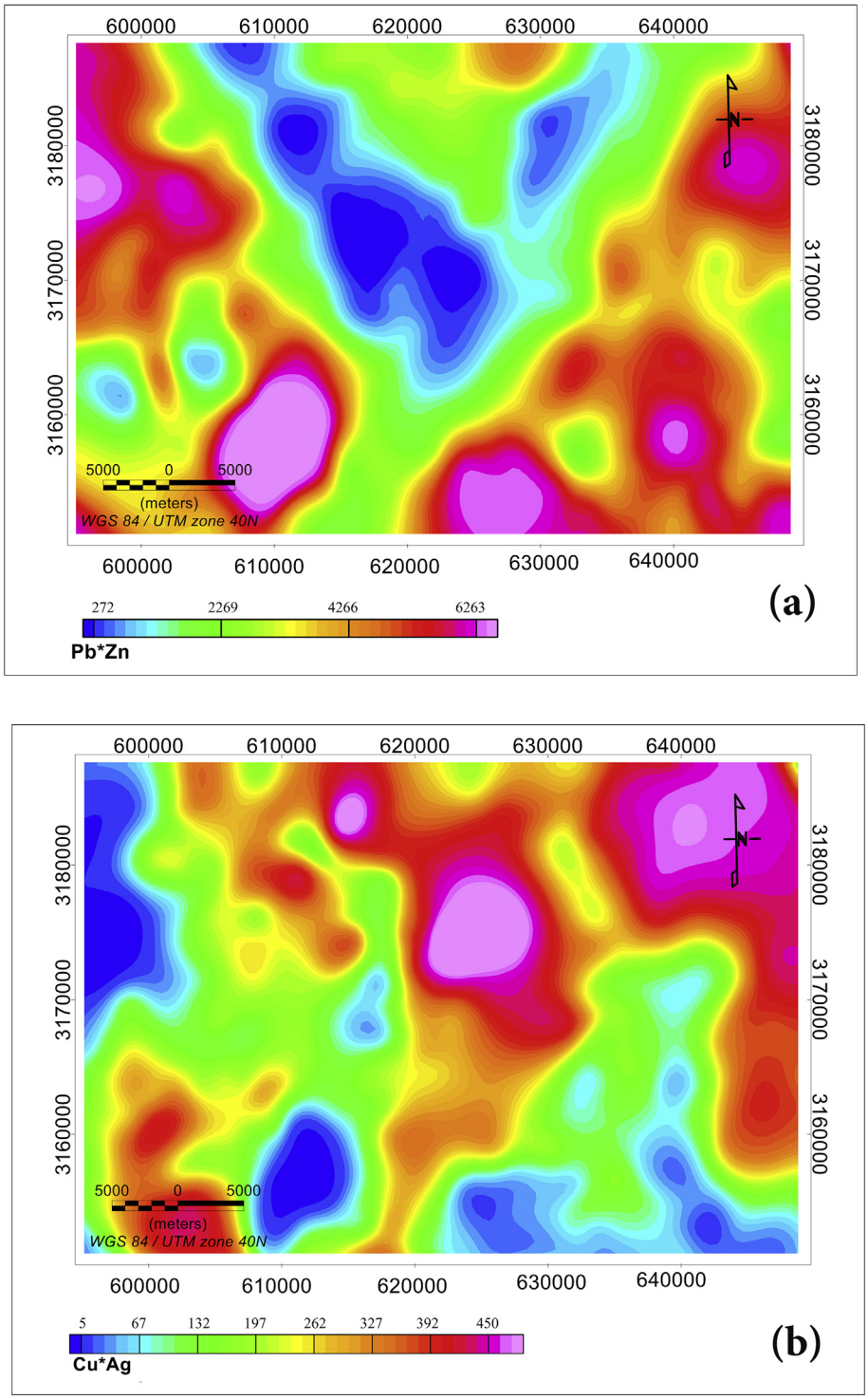


**Fig. 2.** Geochemical map of a) Pb × Zn and b) Cu × Ag in Jebal-Barez.

cross section to represent the geochemical anomaly using the Eq. (4).

$$P = 2L \times \Delta x\left(\sum_{x=1}^{N} C_x - NC_0\right) \quad (4)$$

In Eq. (4), P is the areal productivity; C0 is the background concentration; Cx is the values greater than the anomaly concentration; N is the number of anomal samples; 2 L is the distance between profiles, and Δx is the distance between the samples in each profile (Solovov, 1987).

## 4. Results and discussion

### 4.1. Regional geochemical exploration by G(Vz) model at Jebal-Barez

The multiplied haloes of Cu × Ag are related to the sub-ore mineral deposit, and the multiplied haloes of Pb × Zn are related to the upper-ore mineral deposit in Jebal-Barez (Ziaii et al., 2011). The zonality index map is presented in Fig. 2. Cu × Ag tend to concentrate in the central part of the zone, whereas Pb × Zn have a tendency to concentrate in the surrounding part of Jebal-Barez (Fig. 2).

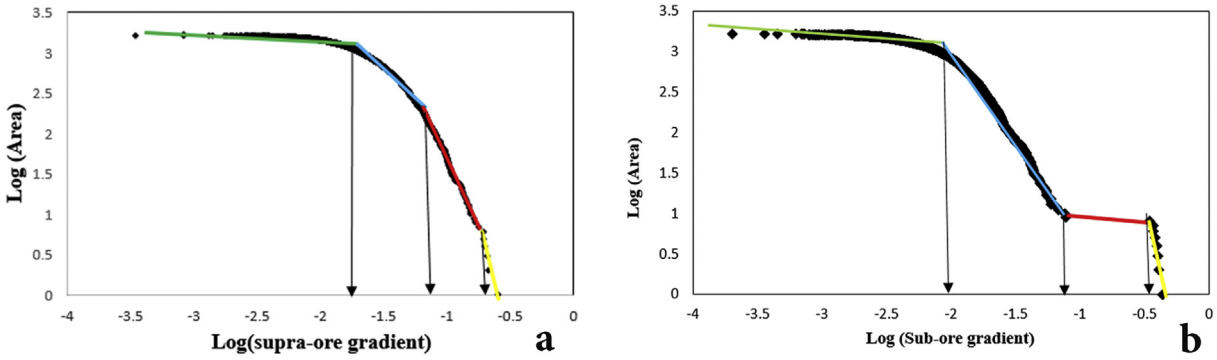


**Fig. 3.** Log-log plot of area versus concentration for a) supra-ore and b) sub-ore elements in Jebal-Barez.

The gradient values for the supra-ore (Pb × Zn) elements and the sub-ore (Cu × Ag) elements were calculated for their distribution, and these values were mapped in Fig. 4. Classification of the gradient values was carried out using the fractal method. A Gr-A plot, as illustrated in Fig. 3, was obtained to reveal the relation between the threshold value and the number of cells with values greater than or equal to it.

Based on these plots, there are three geochemical populations for the supra-ore gradient. The first threshold is 0.02 (log gradient = −1.7) that relates to the low value supra-ore gradient. The second threshold is 0.067 (log gradient = −1.17) that shows a moderate gradient of Pb × Zn in the area. Last populations in the log–log plots reveal a high CG and also show a significant concentration change. Based on the obtained results, the supra-ore gradient map was generated as depicted in Fig. 4.

The Gr-A model consists of sub-ore gradient and the area could be fitted to three straight lines (Fig. 3). The first population is depicted a sub-ore gradient lower than 0.0083, and the medium population shows the relation between the area and the sub-ore CG values ranging from 0.0083 to 0.079. The last population ranging from 0.079 to 0.437 could be interpreted as the sub-ore element anomaly zone.

The CG values for the sub-ore and supra-ore elements were mapped as depicted in Fig. 4. The co-existence of both the supra-ore and sub-ore local maxima implies a blind mineralization (Ziaii et al., 2009). Local anomalies of the supra-ore and sub-ore elements are distinguished in the Jebal-Barez area. According to the local anomalies, four zones were identified in Jebal-barez. A high value of the sub-ore Cu × Ag gradient exists in the center of region in Zone II. The supra-ore gradient value is significant in the west (zone IV) and SW (zone I) of the region. High values of the sub-ore and supra-ore element gradients exist in zone III. The gradient values for the four zones are presented in Table 1.

Zone I was detected as the main blind mineralization in Jebal-Barez that had been previously intersected by drilled borehole for exploration purposes. Ziaii et al. (2011) used the WofE method, and reported sub-area I as the high potential parts for blind mineralization. In addition, Safari et al. (2016) achieved the same results using the fuzzy and singularity method in this region. According to Table 1, the supra-ore gradient (=0.067) is greater than the sub-ore gradient (=0.0133). Also the Pb × Zn surface is above the Cu × Ag surface and the amount of G(Vz) in BM zone is 5.04 (> 1).

The great concentration change of the elements in the geochemical

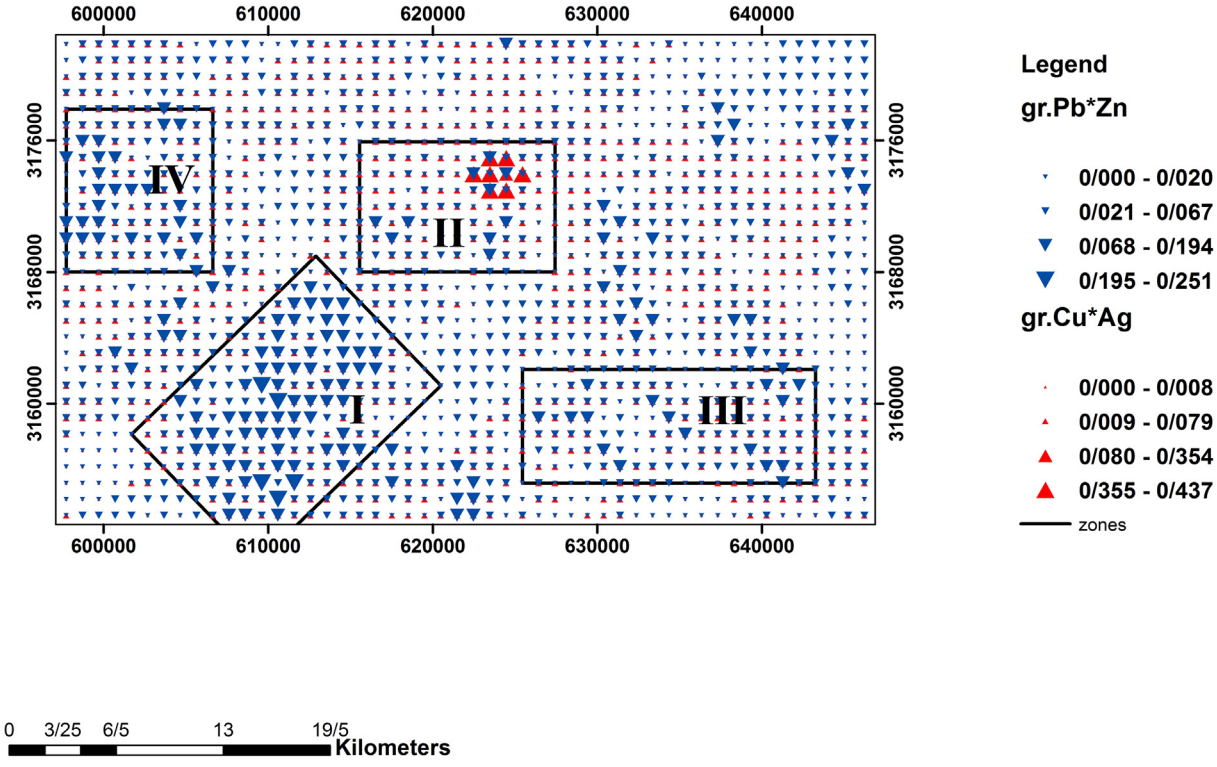


**Fig. 4.** Co-existence of two local maxima for supra-ore and sub-ore elements in Jebal-Barez.

**Table 1**
Identification of geochemical anomaly (IGA) in Jebal-Barez.

| Local anomaly | Zone I | Zone II | Zone III | Zone IV |
|---|---|---|---|---|
| Pb*Zn gradient | 0.067 | 0.0313 | 0.0356 | 0.0466 |
| Cu*Ag gradient | 0.0133 | 0.044 | 0.0127 | 0.0146 |
| G(Vz) | 5.04 > 1 | 0.7 < 1 | 2.8 > 1 | 3.192 > 1 |
| IGA | Blind mineralization | Zone disperse mineralization | Blind mineralization | Blind mineralization |
| Alteration | Porpylitic, argillic, phyllic | Argillic, phyllic | Porpylitic, argillic, phyllic | Porpylitic, argillic, phyllic |

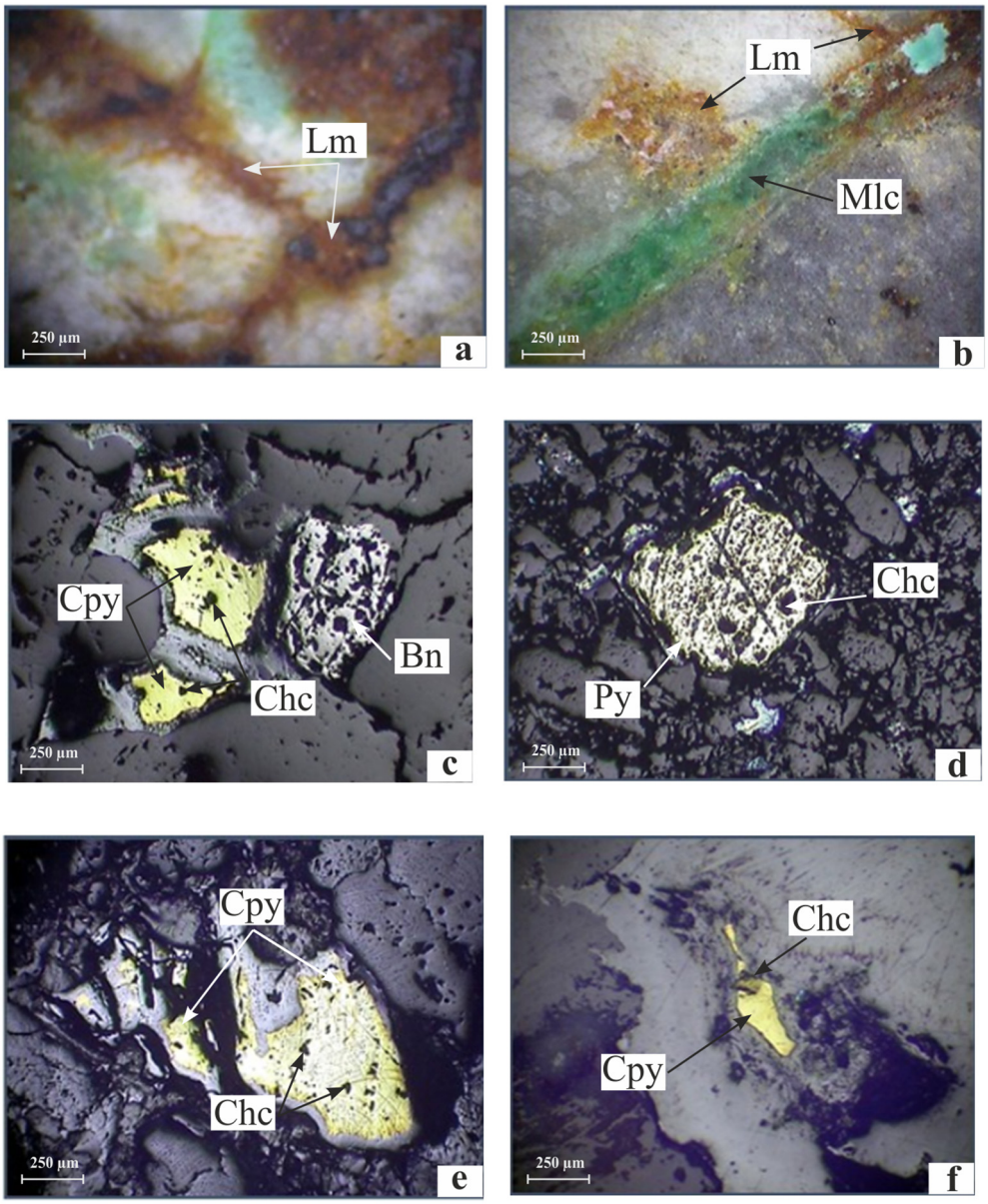


**Fig. 5.** Distribution of economic minerals in thin section and polish section of different samples. a – malachite (Mlc) cross contamination and oxides and hydroxides of iron-containing strains (XPL, 40×); b – the presence of veins Malachite is the result of intrusion of carbonate hydrothermal solution containing copper into the oxide veins (XPL, 40×); c – chalcopyrite (Cpy), chalcocite (Chc) and bornite (Bn) (PPL, 40×); d – present of secondary pyrite with chalcocite (Chc) (PPL, 40×); e and f – chalcopyrite (Cpy) change to the chalcocite (Chc) (PPL,40×).

distribution maps is related to the surfacing anomaly, and the little concentration change is related to a deep geochemical anomaly. The high values for the supra-ore element gradients show that this anomaly is related to the surface, and the low gradient value for the sub-ore elements show that this anomaly is related to the deep anomaly. Therefore, a great value for the supra-ore gradient compared with the sub-ore gradient shows an erosional surface above holes and a probability of blind mineralization.

In the center of Jebal-Barez exist most of the known deposits with outcropping ore body. The erosional surface is in the center of haloes with outcropping weak mineralization in the zone II location. G(vz) in this zone is 0.7(< 1). Therefore, in the next stage of exploration processing, the presented deduction model was used, and the research work was focused on SW of Jebal-Barez as a high favourability of blind

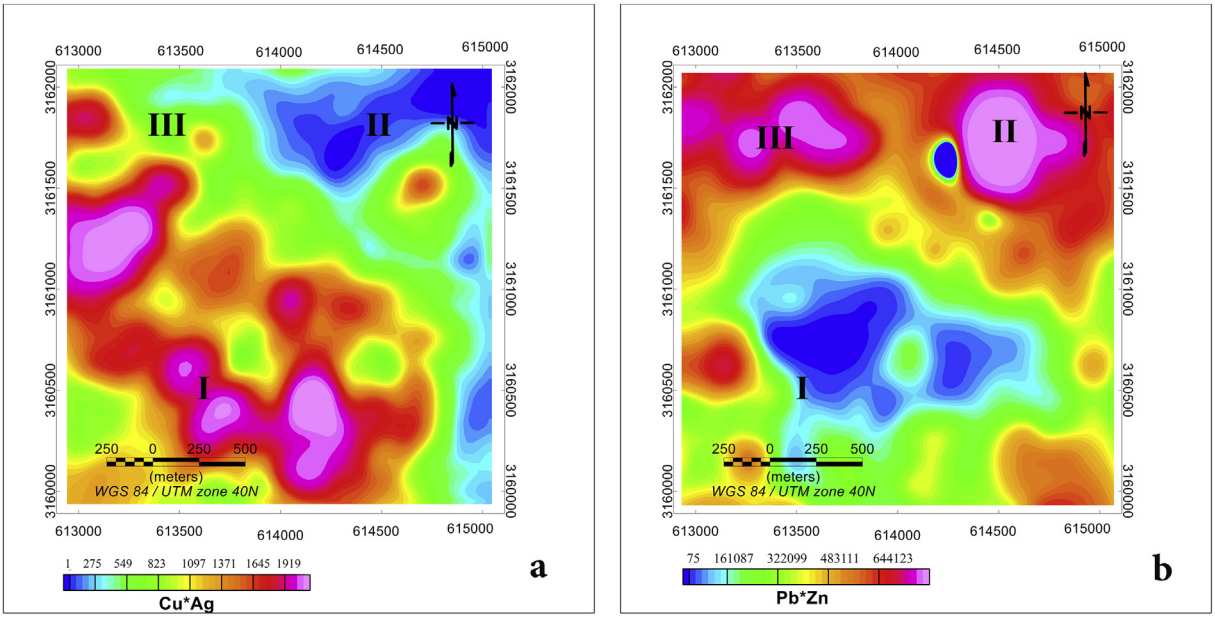


**Fig. 6.** Geochemical map of a) Cu × Ag and b) Pb × Zn in Kerver1.

**Table 2**
Areal productivity and zonality index of case studies compared with Sungun and Astamal.

| | $\frac{P(Pb)*P(Zn)}{P(Cu)*P(Mo)}$ | $\frac{P(Pb)*P(Zn)}{P(Cu)*P(Ag)}$ | P(Cu) | P(Ag) | P(Mo) | P(Pb) | P(Zn) |
|---|---|---|---|---|---|---|---|
| Astamal | 0.45 | – | 2584 | – | 266 | 166 | 1891 |
| Sungun1 | 8.1 | 77 | 15,271 | 22.8 | 1001 | 17,499 | 7146 |
| Sungun2 | 73.2 | 826 | 3285 | 19.7 | 221.9 | 12,379 | 4315 |
| Anomaly I-Kerver1 | 0.07 | 3.5 | 52,649 | 40 | 2008 | 2178 | 3398 |
| Anomaly II-Kerver1 | 80 | 597 | 11,523 | 3 | 25 | 2666 | 8678 |
| Anomaly III-Kerver1 | 27 | 146 | 7203 | 18 | 93.35 | 2152 | 2753 |
| Anomaly I-Kerver2 | 0.05 | 2.4 | 169,670 | 61.1 | 2829 | 3246 | 737 |
| Anomaly II-Kerver2 | 2.6 | 84.6 | 17,726 | 6.5 | 221.4 | 1243 | 7843 |
| Anomaly III-Kerver2 | 1 | 17.9 | 24,548 | 8.8 | 157 | 1915 | 2021 |
| Anomaly I-Kerver3 | 23.2 | 407 | 23,110 | 51.6 | 906.56 | 7993 | 60,711 |
| Anomaly II-Kerver3 | 44.6 | 609 | 5774 | 40.2 | 549.12 | 5964 | 23,753 |
| Anomaly III-Kerver3 | 152 | 1893 | 578.5 | 7.44 | 92.6 | 1378 | 5915.5 |
| Anomaly I-Kerver4 | 540.7 | 2151 | 1316 | 1.9 | 7.56 | 3284 | 1638 |
| Anomaly II-Kerver4 | – | – | 3621 | 1.26 | 434.8 | 634.5 | – |
| Anomaly III-Kerver4 | – | – | 421.4 | 5.6 | 68.31 | 1022.4 | – |

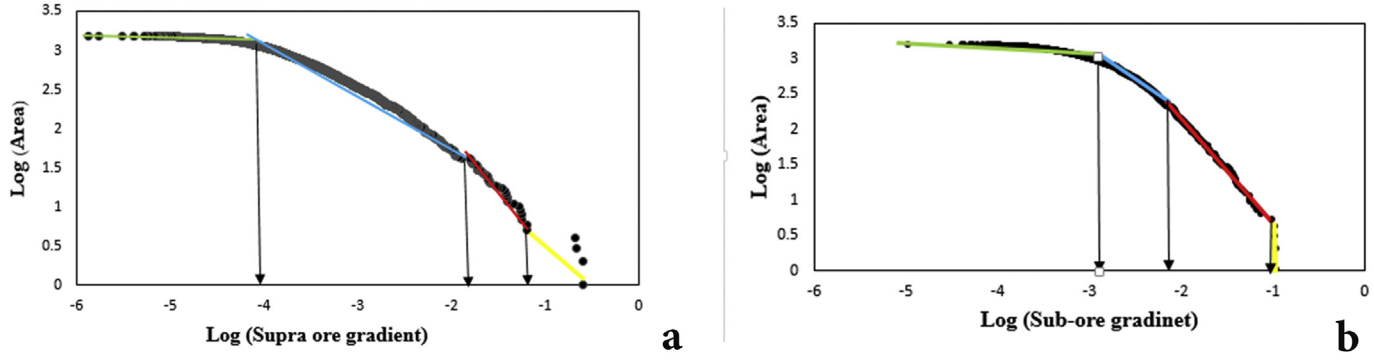


**Fig. 7.** Log-log plot of area versus concentration a) supra-ore and b) sub-ore elements in Kerver1.

mineralization in this region.

The initial field investigation shows that there are various indicators of porphyry copper mineralization in and around the target areas. Meanwhile, thin sectional and polished sectional study show that the copper minerals include Pyrite, Malachite, Azurite, Chalcopyrite, Bornite, iron oxide. Hematite can be seen in veins-veinlets which cut the cross (Fig. 5a). Present activities of Limonite is obvious mainly around the veins of Hematite (Fig. 5b). Presence of Malachite is not very noticeable. Malachite can be seen around veins of iron oxide (Limonite) (Fig. 5b). There is Chalcopyrite in the form of primitive and secondary Chalcocite has created by the effect of alteration on Chalcopyrite (Fig. 5e and f). Bornite exist in the form of primitive and

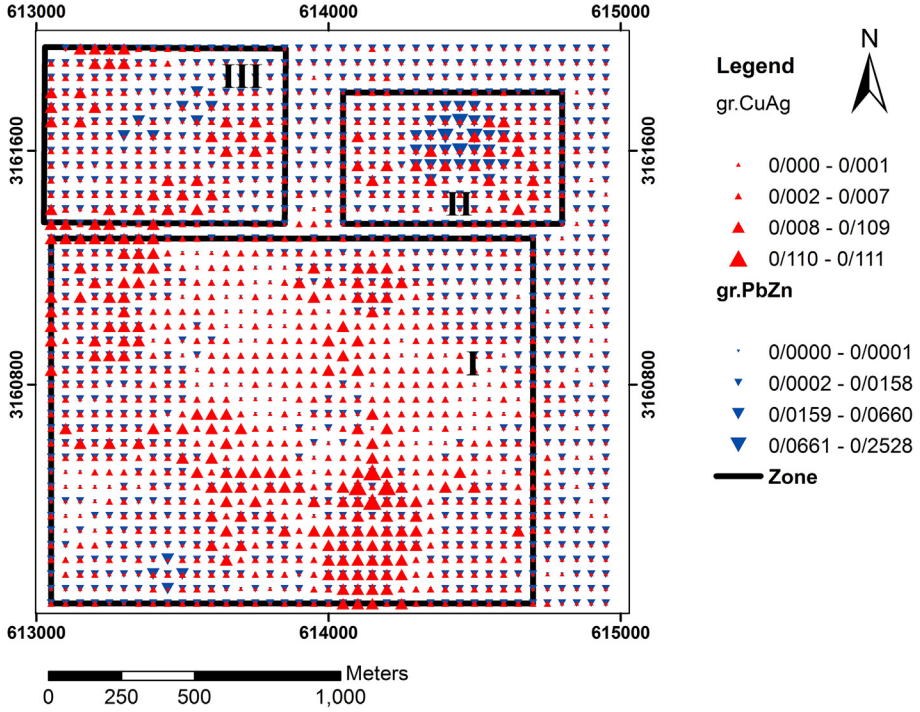


**Fig. 8.** Co-existence of two local maxima for supra-ore and sub-ore elements in Kerver1.

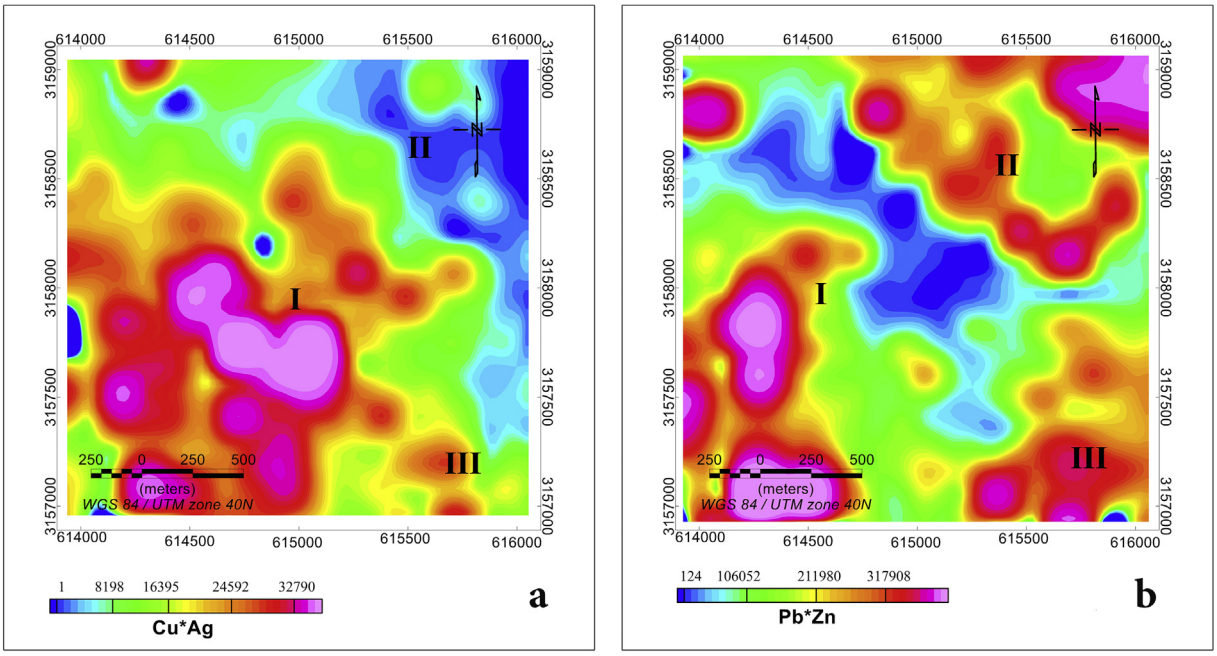


**Fig. 9.** Geochemical map of a) Cu × Ag and b)Pb × Zn in Kerver2.

ordinary they are automorf. This minerals change to Chalcocite from the around and along the discontinued surfaces (Fig. 5c). Pyrite are in two forms. The first one has been replaced by the iron hydroxide and second, they have informed and sporadic texture in which no alteration and replacement can be detected (Fig. 5d).

### 4.2. Local geochemical exploration by G(Vz) model at Kerver area

The geochemical data uninfluenced by the mineralization processes describe the local geochemical background variation, and the anomalous results provide targets for assessment of mineral potential by drilling in a local scale (Demetriades et al., 2015).

A geochemical exploration was carried out in the sub-area suggested in the previous section. For this purpose, a local scale exploration was implemented in Kerver1 (Baggolom), Kerver2, Kerver3, and Kerver4 in this area (Figs. 1 and 2). Local exploration was carried out using the CG method.

#### 4.2.1. Local exploration in kerver1

Distribution of the supra-ore elements (Pb × Zn) and sub-ore elements (Cu × Ag) of kerver1 are illustrated in Fig. 6. A significant anomaly of Pb × Zn is in the north of Kerver1. The value for Cu × Ag is

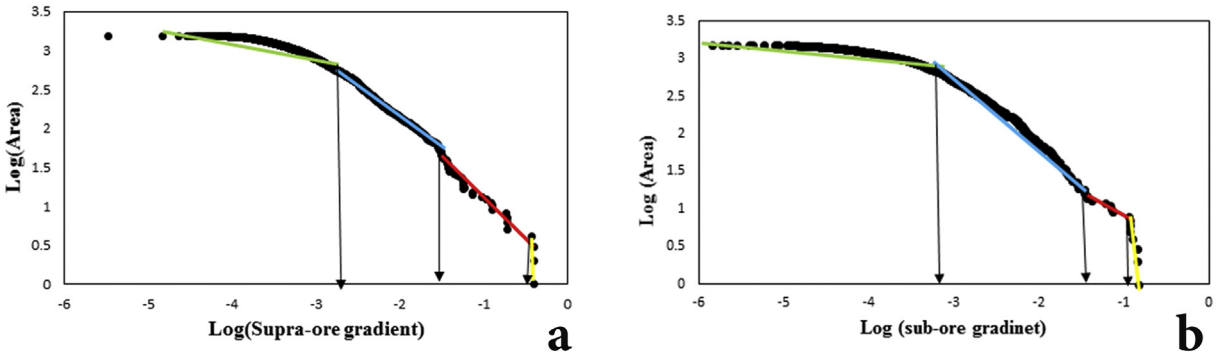


**Fig. 10.** Log-log plot of area versus concentration of a) supra-ore and b) sub-ore elements in Kerver2.

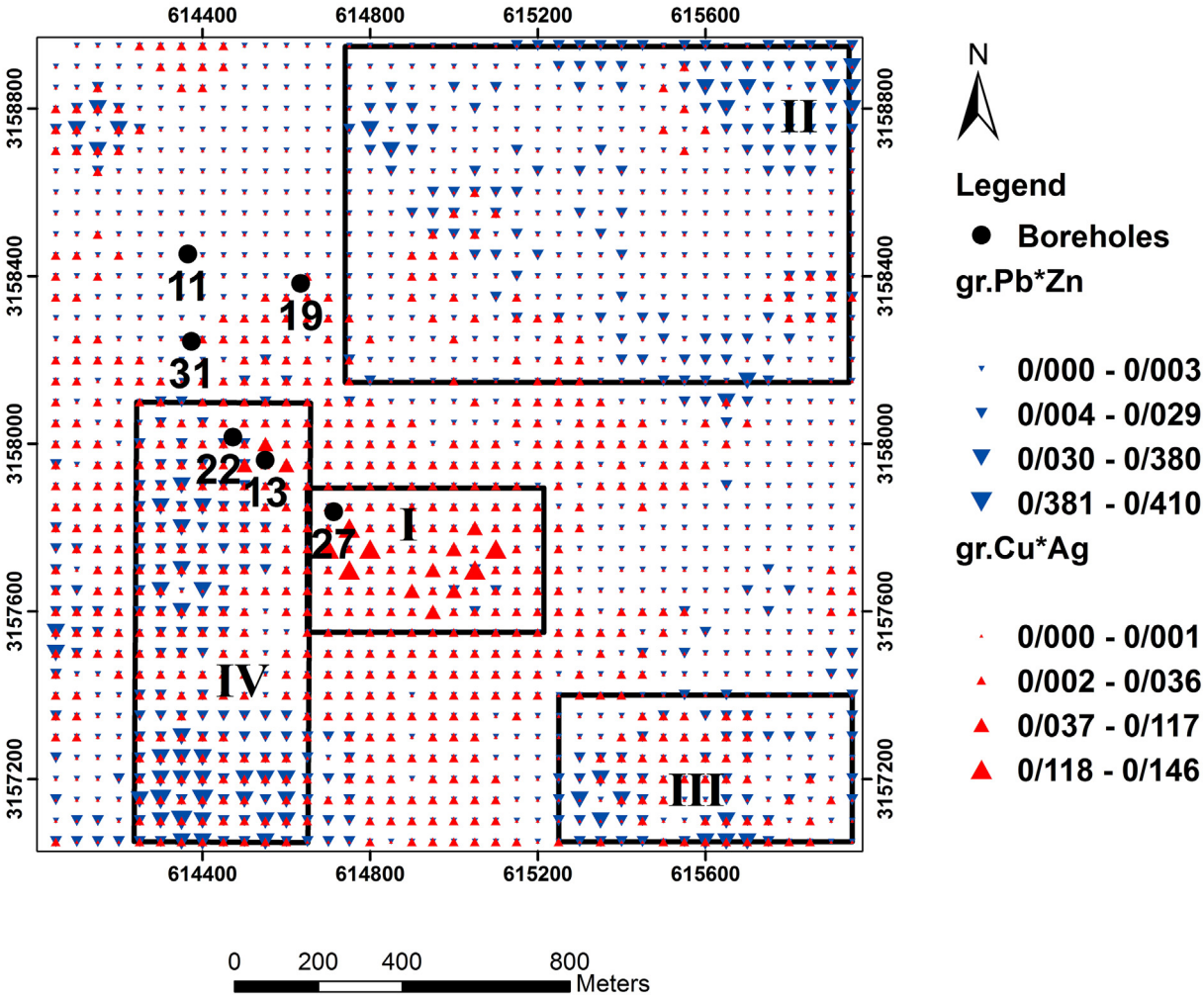


**Fig. 11.** Co-existence of two local maxima for supra-ore and sub-ore elements in Kerver2.

high in SW of this area.

Three local anomalies of the sub-ore and supra-ore elements were detected in this area. Areal productivity and vertical zonality index were calculated in these local anomalies.

The productivities of the Pb, Zn, Cu, Ag, and Mo elements were calculated using Eq. (4). Then zonality indices for Pb × Zn/Cu × Ag and Pb × Zn/Cu × Mo were calculated with the productivity of the elements. The obtained values were compared with the ones presented by the vertical zonality model by Ziaii, 2008(refer to Fig. 1 in Ziaii et al., 2011).

The zonality indices for Pb × Zn/Cu × Mo and Pb × Zn/Cu × Ag in anomaly I of Kerver1 were 0.07 and 3.5, respectively (Table 2). According to the vertical zonality model, above the surface of this anomaly was eroded. Borna and Sodishoar (2005) compared the vertical zonality index of each zone with this value in the Sungun and Astamal areas. Sungun and Astamal are located in NW of Iran, and they are known as the blind and zone disperse mineralizations, respectively. There is no analysis of Ag concentration in Astamal, and thus the zonality index was calculated for Pb × Zn/Cu × Mo in this area. According to this comparison, Borna and Sodishoar (2005) have reported that mineralization in zone I is disperse and non-economic, whereas blind mineralization exists in zones II and III of Kerver1. According to

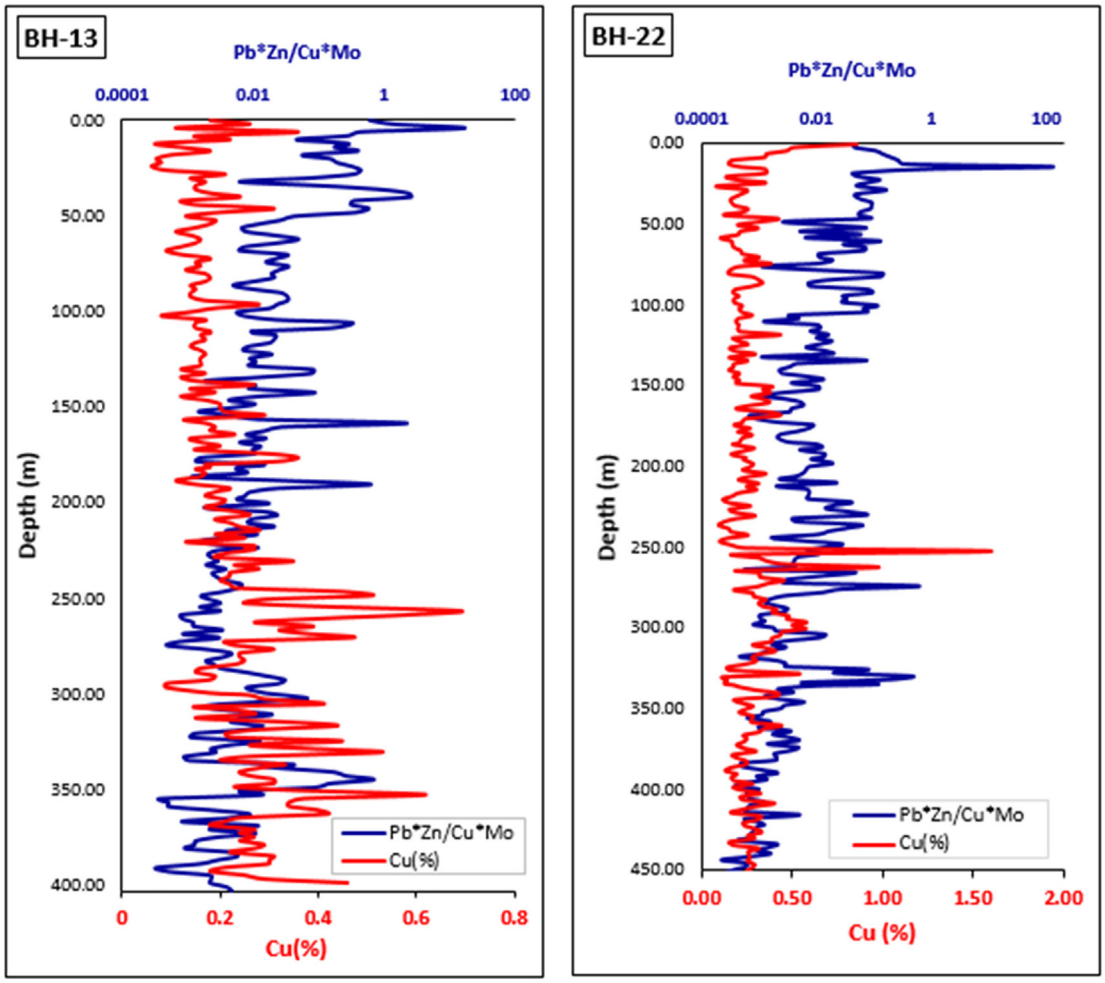


**Fig. 12.** Variations of Cu concentration (%) and vertical zonality index Log (Pb × Zn/Cu × Mo) in depth for boreholes 13 and 22.

the vertical zonality model, the eroded surface is located above the mineralization of II and III. In this study, detection of mineralization was done using the gradient values.

The gradient values of the sub-ore and supra-ore elements were calculated in the xy direction according to Eqs. (2) and (3) in Matlab Software programming in Kerver1. The obtained values were mapped in Fig. 8.

Classification of values were done using the fractal method. According to this method, the supra-ore gradient and sub-ore gradient values were classified into the three classes (Fig. 7).

Three local anomalies of the sub-ore and supra-ore gradients were recognized in the gradient map. The average of concentration gradients in each local anomaly was calculated, and the obtained values were presented in Table 3. The sub-ore gradient value was higher than the supra-ore value in zones I and III. Therefore, the sub-ore element surface is upper than the supra-ore element surface for all zones, and they are the ZDM. The overlap of the two-phase mineralization is probable in zone III, which is called multiformation (Borna and Sodishoar, 2005).

The supra-ore gradient and sub-ore gradient values were 0.0144 and 0.0042, respectively, in zone II. G(vz) in this zone was 3.43 (> 1). Distributions of Pb × Zn and Cu × Ag are related to the surface and depth of ground surface respectively, and zone II is BM. This anomaly is located on the diorite, subvolcanic (micro diorite) unit of geology (Fig. 1).

### 4.2.2. Local exploration in Kerver2 area

High values of the supra-ore elements (Pb × Zn) can be detected in the north and SW of provenances, and high values of the sub-ore elements (Cu × Ag) was happened in the central area and SW of the area (Fig. 9). Borna and Sodishoar (2005) investigated concentration path finder elements, and recognized three anomalies in this area. According to their study, two anomalies (II and III) located in the eastern side of the area, which are blind mineralization, and the anomaly located in the west half (I) of the area is a zone of disperse mineralization. The areal productivity and vertical zonality of these local anomalies are presented in Table 2. Comparison of the zonality indices in this table with vertical zonality model presented the same result as Borna and Sodishoar (2005). In this study, identification of the geochemical anomalies was done using the gradient values.

CG was calculated for two distribution functions of Cu × Ag and Pb × Zn in the x and y directions in Kerver2. The obtained CG values were classified using the fractal method for the supra-ore and sub-ore elements. Threshold of the gradient values was indicated in the fractal graph (Fig. 10).

The spatial distribution patterns for the sub-ore and supra-ore gradients were shown in the geochemical map (Fig. 11). According to the gradient map, four local anomalies were recognized in Kerver2. The average CG of the supra-ore and sub-ore elements were calculated for each zone (Table 4).

The CG values for the supra-ore elements were higher than those for the sub-ore elements in zones II and III. The G(Vz) values in these zones were 11.4 and 6.3, respectively. Therefore, the surface anomaly for Pb × Zn is above the surface of Cu × Ag, and BM exists in zones II and III. The obtained results using the gradient method are in agreement with the obtained results by Borna and Sodishoar (2005) in zones II and III. The geological units in zone II and III are granodiorite with diorite

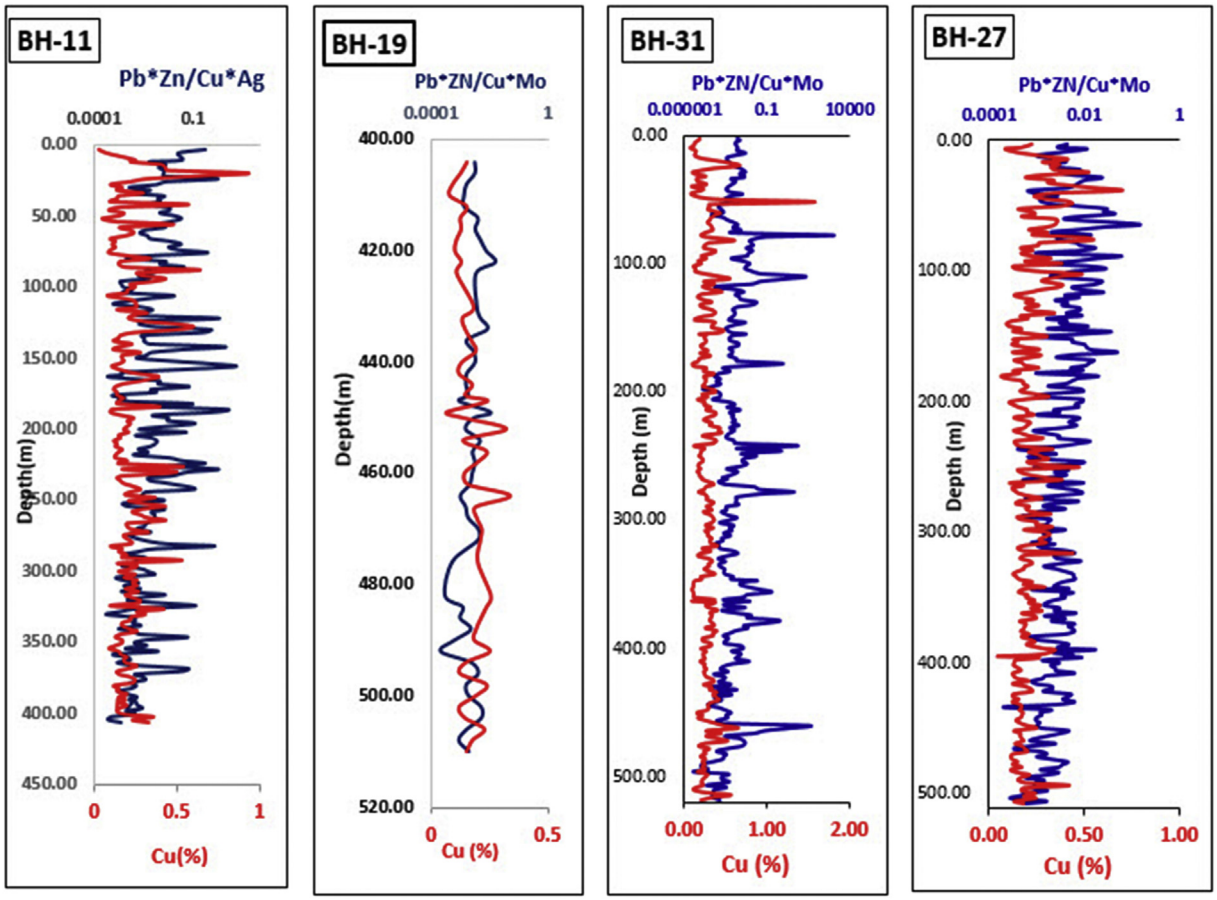


**Fig. 13.** Variations in Cu concentration (%) and vertical zonality index log (Pb × Zn/Cu × Mo) in depth for boreholes of 11, 19, 27, and 31.

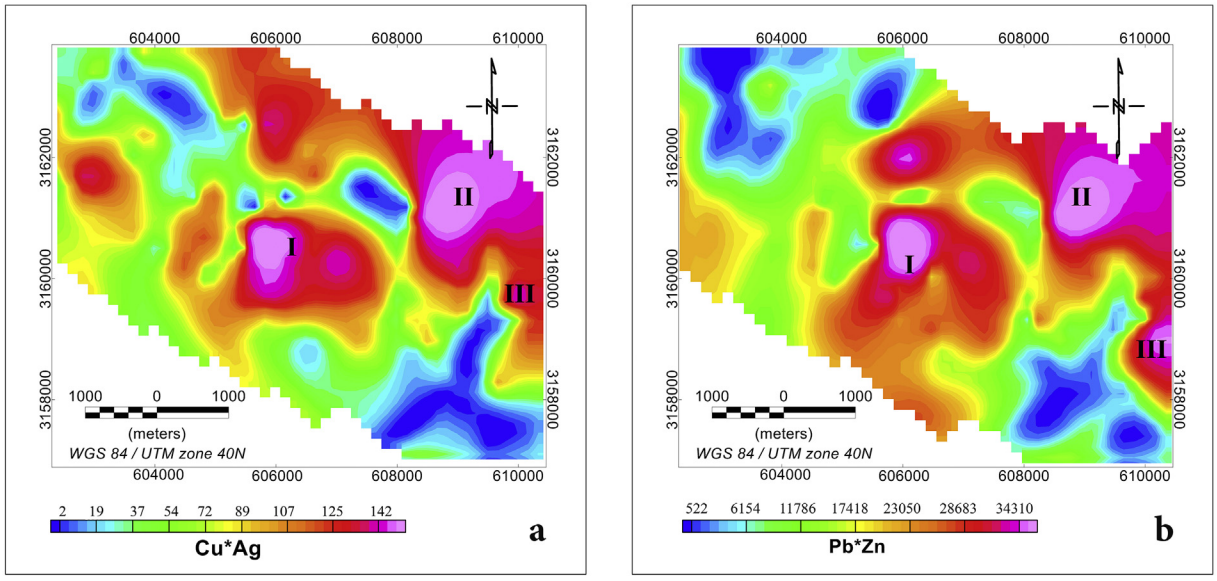


**Fig. 14.** Geochemical map of a) Cu × Ag and b)Pb × Zn in Kerver3.

varying composition and texture, diorite, subvolcanic with granodiorite dykes (Fig. 1). Borna and Sodishoar (2005) reported the western half of Kerver2 as zone disperse mineralization, whereas the two drilled boreholes of 13 and 22 in this part of the area show the economic mineralization in depth. According to the variation in the vertical zonality index (Pb × Zn/Cu × Ag), in bore hole 22, the value for this index is high near the surface (=133) while it was gradually decreased (=0.0025) toward the depth of 450 m, whereas Cu concentration was increased from the surface to a depth of 250 m. In borehole 13, the zonality index decreases, while the Cu concentration increases to a depth of 350 m.

According to the gradient map, two zones were recognized in the western side of the area (Fig. 11). The drilled boreholes of 13 and 22 (Fig. 12) are located in zone IV. Ratio of the supra-ore gradient to the

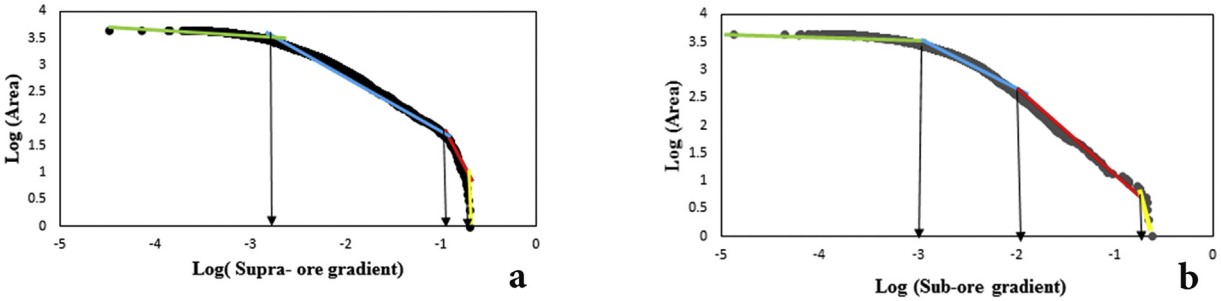


**Fig. 15.** Log-log plot of area versus concentration of a) supra-ore and b) sub-ore elements in Kerver3.

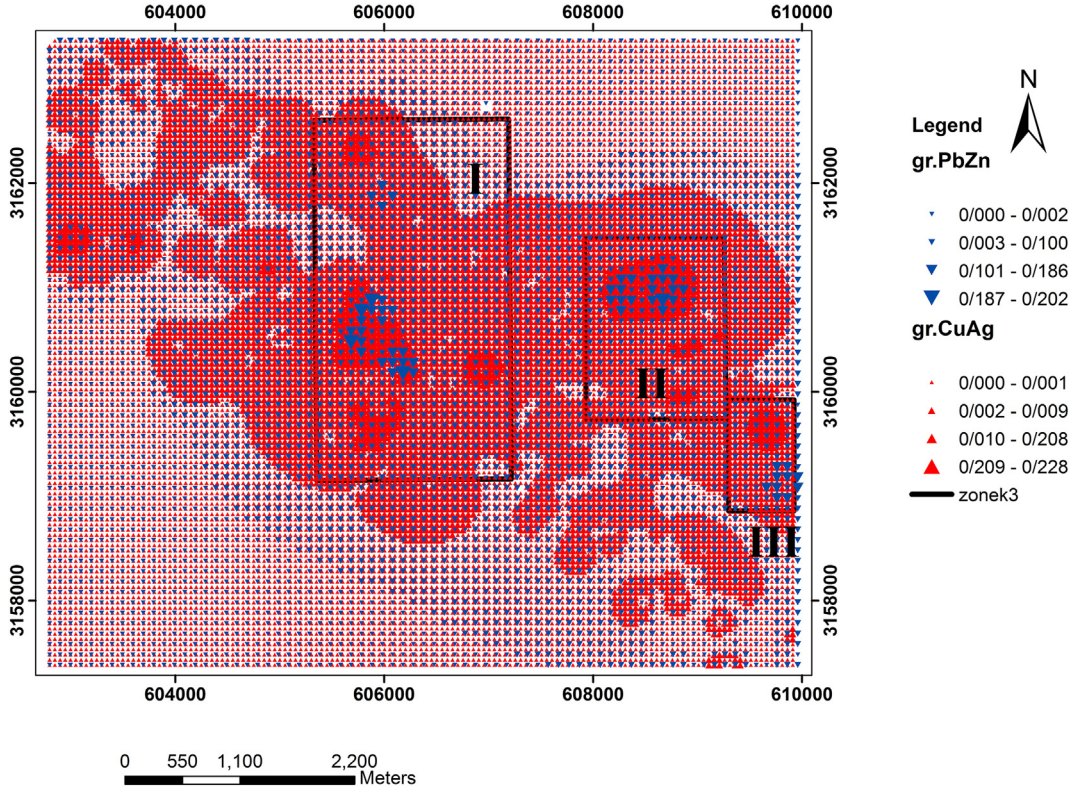


**Fig. 16.** Co-existence of two local maxima for a) supra-ore and b) sub-ore elements in Kerver3.

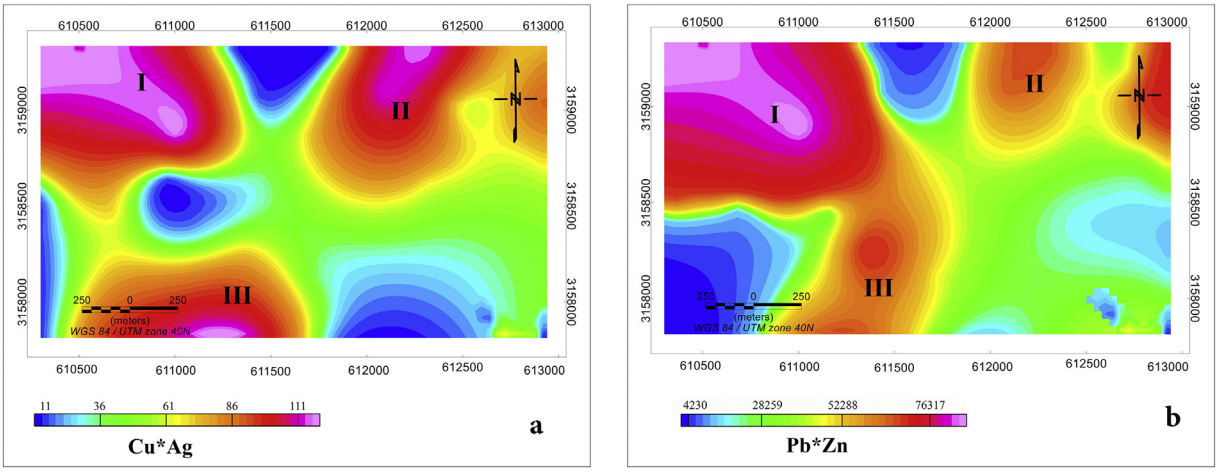


**Fig. 17.** Geochemical map of a) Cu × Ag and b) Pb × Zn in Kerver4.

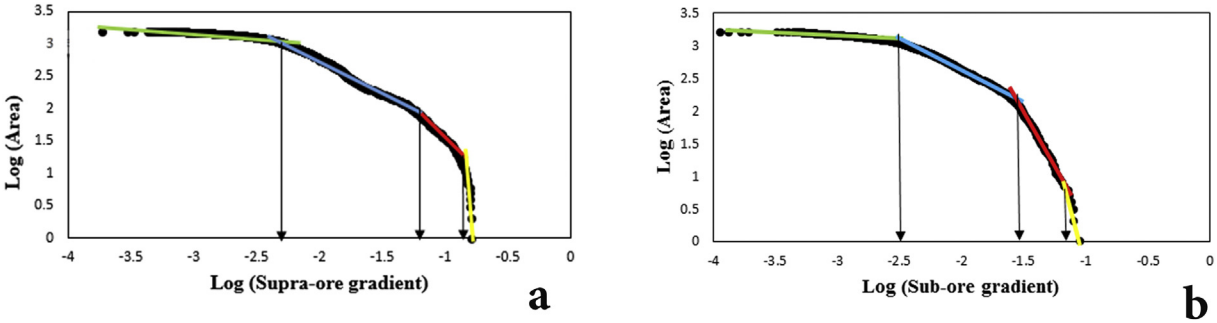


**Fig. 18.** Log-log plot of area versus concentration of a) supra-ore and b)sub-ore elements in Kerver4.

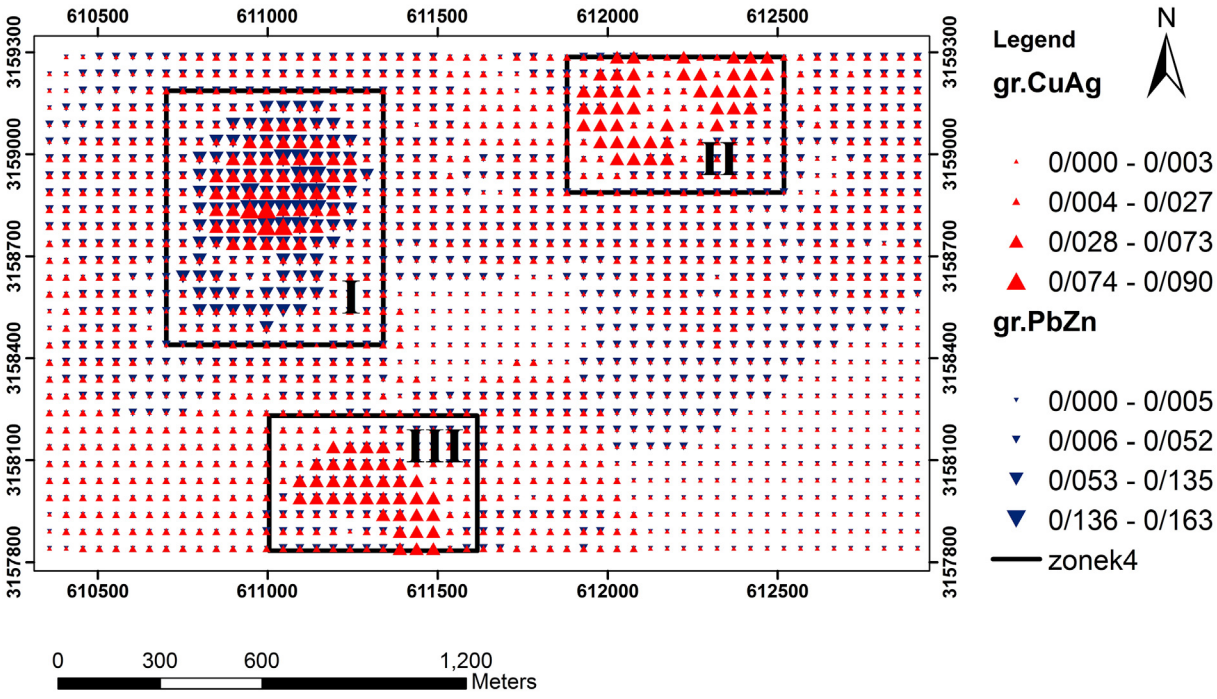


**Fig. 19.** Co-existence of two local maxima for supra-ore and sub-ore elements in Kerver4.

**Table 3**
Identification of Geochemical Anomaly (IGA) in Anomaly Geochemical Field (AGF) in Kerver1.

| | Anomaly I | Anomaly II | Anomaly III |
|---|---|---|---|
| Pb*Zn | 0.0004 | 0.0144 | 0.0024 |
| Cu*Ag | 0.0052 | 0.0042 | 0.0053 |
| G(Vz) | 0.077 | 3.43 | 0.45 |
| IGA | Zone disperse mineralization | Blind mineralization | Zone disperse mineralization |
| Alteration | Potassic, sericite, argillic, propilitic | No alteration | No alteration |

**Table 4**
Identification of Geochemical Anomaly (IGA) in Anomaly Geochemical Field (AGF) in Kerver2.

| | Anomaly I | Anomaly II | Anomaly III | Anomaly IV |
|---|---|---|---|---|
| Pb*Zn | 0.0006 | 0.004 | 0.0057 | 0.024 |
| Cu*Ag | 0.021 | 0.00035 | 0.0009 | 0.0042 |
| G(Vz) | 0.03 | 11.4 | 6.3 | 5.7 |
| IGA | Zone disperse mineralization | Blind mineralization | Blind mineralization | Blind mineralization |
| Alteration | Sericite | No alteration | No alteration | Sericite, propilitic, |

**Table 5**
Identification of Geochemical Anomaly (IGA) in Anomaly Geochemical Field (AGF) in Kerver3.

| | Anomaly I | Anomaly II | Anomaly III |
|---|---|---|---|
| Pb*Zn | 0.02 | 0.03 | 0.018 |
| Cu*Ag | 0.0056 | 0.008 | 0.004 |
| G(Vz) | 3.57 | 3.75 | 4.47 |
| IGA | Blind mineralization | Blind mineralization | Blind mineralization |
| Alteration | No alteration | No alteration | No alteration |

**Table 6**
Identification of Geochemical Anomaly (IGA) in Anomaly Geochemical Field (AGF) in Kerver4.

| | Anomaly I | Anomaly II | Anomaly III |
|---|---|---|---|
| Pb*Zn | 0.0586 | 0.0063 | 0.0069 |
| Cu*Ag | 0.019 | 0.022 | 0.022 |
| G(Vz) | 3.08 | 0.28 | 0.3 |
| IGA | Blind mineralization | Zone disperse mineralization | Zone disperse mineralization |
| Alteration | No alteration | No alteration | No alteration |

sub-ore gradient in this zone is higher than 1 (G(Vz) = 5.7). Gradient value introduces the zone IV as a blind mineralization but the zonality method could not detect BM in this zone. Units of geology in zone IV are granite, diorite, microgranodiorite, alkali granite with dykes (Fig. 1) G(Vz) in zone I is lower than 1, and the sub-ore gradient is lower than the supra-ore gradient. Zone I is located on the recent alluvium and diorite subvolcanic units geology (Fig. 1).

The G(vz) value in zone I shows that this zone is ZDM. The distribution of the vertical zonality indices for (Pb × Zn/Cu × Mo) in the drilled borehole of 27 in zone I is illustrated in Fig. 13. The vertical zonality value is constant from the surface to the depth, and a high concentration of Cu exists near the surface. The three boreholes of 31, 11, and 19 are located in the western part of Kerver2. These boreholes were drilled outside the anomaly geochemical field. The vertical zonality index in these bore holes are almost constant from surface to the depth (Fig. 13). The Cu concentration in these boreholes are significant near the surface, and decreases to the depth. Variation in the vertical zonality and Cu concentration in these boreholes shows that these boreholes were drilled in the disperse mineralization zone.

#### 4.2.3. Local exploration in Kerver3 area

High values of supra-ore concentration (Pb × Zn) exist in the east and central sides of the area. Concentration of the sub-ore elements (Cu × Ag) is significant in the centre and east of Kerver3 (Fig. 14). Three local anomalies of the sub-ore and supra-ore elements were detected in Kerver3. The areal productivity and vertical zonality indices are presented in Table 2. The vertical zonality index is significant compared with this value in the blind porphyry copper mineralization of the case studies. These values, compared with the zonality model, show that these local anomalies are blind mineralization.

The gradient values for Pb × Zn and Cu × Ag were calculated and illustrated in Fig. 16. The gradient values were classified into three groups using the fractal method (Fig. 15).

Co-existence of the sub-ore and supra-ore gradient values is shown in Fig. 16. Three local anomalies were recognized in this map. The gradient values for these zones were tabulated in Table 5. The gradient values for the supra-ore gradient were higher than those for the sub-ore gradient in these zones, and the G(Vz) values were 3.57, 3.75, and 4.47, respectively. The G(Vz) values for these zones are > 1, and therefore, Pb × Zn in these zones are upper than the Cu × Ag surface. The CG model suggested the presence of a blind mineral deposit in the Kerver3 area. More investigation is required for drilling boreholes in this area. Existence of blind mineralization is more probable in zone 3. The geological units in Kerver3 are altered andesite, andesitic tuff, dykes of microdiorite, granite to diorite, and alkali granite with partly alteration dykes of diabase, green-black well bedded tuff, sandstone, andesite, black andesite and silicified andesite with few iron oxide.

#### 4.2.4. Local exploration in Kerver4 area

Distributions of the supra-ore elements (Pb × Zn) and sub-ore elements (Cu × Ag) are illustrated in Fig. 17. High anomaly of Cu × Ag exist in the west and NE of Kerver4, and the Pb × Zn value is high in NW of this area. Three local anomalies of the sub-ore and supra-ore elements were detected in Kerver4. The areal productivity and vertical zonality index for these local anomalies were tabulated in Table 2. The vertical zonality indices for Pb × Zn/Cu × Ag and Pb × Zn/Cu × Mo in anomaly I of Kerver4 are significant, being equal to 2151 and 540.7, respectively (Table 2). According to the vertical zonality model, these values show existence of a blind mineralization in local anomaly I. On the other hand, anomaly of Pb × Zn in these two anomalies is weak and concentration of Cu in these anomalies are 0.03% and 0.01%, respectively, which show that these anomalies are non-economic and zone disperse mineralization.

The gradient values for these distributions were calculated, and classified using the fractal method (Fig. 18). The gradient map of these distributions is shown in Fig. 19. According to this map, three zones were detected in Kerver4. The sub-ore and supra-ore gradient values are presented in Table 6.

The gradient value for Pb × Zn (=0.0586) is 3.08 times higher than the Cu × Ag gradient (=0.019) in zone I. Therefore, there is a blind mineralization in this zone of Kerver4. The geology of units in zone I are altered andesite, andesitic tuff, dykes of microdiorite and red bedded of pyroclastics, sandstone, rhyolitic agglomerate and andesite tuff. Ratios of supra-ore gradient to the sub-ore gradient are 0.28 and 0.3 in zones II and III. These values show that these zones are ZDM, and there is no economic mineralization in these zones.

Gradient is an important characteristic parameter in geochemical field undoubtedly. Element concentration gradient in geochemical distribution maps shows concentration element change. High value are related to the surface anomaly and vice versa. Concentration gradient of sub-ore elements and supra-ore elements can help to detect the blind mineralization from zone dispersed mineralization.

## 5. Conclusions

In this research, the G(Vz) index has been applied in concentration gradient analysis for porphyry copper deposits in regional scale of Jebal-Barez. According to the previous research, the SW of Jebal-Barez is a high potential zone for exploration of blind mineralization and detected Kerver as the main blind mineralization. The G(Vz) value in this zone is higher than1.0 and supra-ore gradient is higher than sub-ore gradient value in kerver area. Furthermore, SW of Jebal-Barez was detected as a high potential zone by the G(Vz) model. Consequently, the research focused on four areas in this zone. A favourable location of blind mineralization has been detected by the zonality method in the previous research in Kerver1 and 2. The G(Vz) values in these zones were higher than 1.0. If the average concentration gradient of the supra-ore elements is higher than this value for the sub-ore elements, the anomaly is BM. If the ratio of CG for supra elements is lower than 1.0, the anomaly is a zone of dispersed mineralization.

This study revealed that concentration gradient could be applied to the multivariate recognition of lithogeochemical anomalies and separation of the two types of anomalies ZDM and BM. It was shown that the results obtained by the proposed technique improved those results obtained by the traditional method, significantly. The results obtained by the proposed method were confirmed by drilling bore-holes in Kerver2.

## Acknowledgments

This research was funded by the School of Mining, Petroleum and Geophysics, at the Shahrood University of Technology. Laboratory investigations were carried out at Tomsk Polytechnic University within the framework of a Tomsk Polytechnic University Competitiveness Enhancement Program grant. The authors are grateful to N.P. Laverov, Yu. G. Safonov for their useful suggestions which helped us to improve the mining geochemistry and introducing a new branch of it. Authors are thankful to the anonymous reviewers and the editor for constructive criticisms and useful suggestions on earlier version of the manuscript.

## References

Afaghi, A., Sidjedi, T., Salack, M.M., Stamenkovic, D., 1959. Geological map of Jebal-Barez. Geological survey of Iran. Sheet No. 7647, scale 1:100,000.

Afzal, P., Alghalandis, Y.F., Khakzad, A., Moarefvand, P., Omran, N.R., 2011. Delineation of mineralization zones in porphyry Cu deposits by fractal concentration–volume modeling. J. Geochem. Explor. 108, 220–232.

Bedakhshan, G.H., Sodishoar, P., 2000. Geochemical exploratory exploration in block 2 (JebalBarez, Sabzevaran, Hana). In: National Iranian Copper Industries Company (NICICO) Reports.

Beus, A.A., Grigorian, S.V., 1977. Geochemistry Exploration Methods for Mineral Deposit. Applied Publishing House, Wilmette.

Bingli, L., Xueqiu, W., Ke, G., Li, Z., 2013. The Application of Nonlinear Method in Exploration Geochemistry. Acta Geol. Sin. 87, 726–729.

Borna, B., Sodishoar, P., 2005. Primary exploration of copper in Kerver. In: National Iranian Copper Industries Company (NICICO) Reports.
Chen, Z., Chen, J., Tian, Sh., Xu, B., 2017. Application of fractal content-gradient method for delineating geochemical anomalies associated with copper occurrences in the Yangla ore field, China. Geosci. Front. 8 (1), 189–197.
Cheng, Q., 1999. Spatial and scaling modelling for geochemical anomaly separation. J. Geochem. Explor. 65 (3), 175–194.
Cheng, Q., Agterberg, F.P., Ballantyne, S.B., 1994. The separation of geochemical anomalies from background by fractal methods. J. Geochem. Explor. 51 (2), 109–130.
Cheng, Q., Agterberg, F.P., Bonham-Carter, G.F., 1996. A spatial analysis method for geochemical anomaly separation. J. Geochem. Explor. 56 (3), 183–195.
Cheng, Z., Yao, W., Feng, J., Zhang, Q., Fang, J., 2014. Multi-element geochemical mapping in Southern China. J. Geochem. Explor. 139, 183–192.
Demetriades, A., Birke, M., Albanese, S., Schoeters, I., De Vivo, B., 2015. Continental, regional and local scale geochemical mapping. J. Geochem. Explor. 154, 1–5.
Dorri, M. B. 2006 “Geological and exploration map of Kerver area”, map No, 2. Scale, 1:20000, Geological survey of Iran.
Ghorbani, M., 2013. The Economic Geology of Iran Mineral Deposits and Natural Resources. Springer Science Business Media, Dordrecht (581 p).
Gonzalez, R., Richard, W., 2002. Digital Image Processing, 3rd ed. Upper Saddle River, New Jersey.
Govett, G.J.S., Goodfellow, W.D., Chapman, C., Chork, C.Y., 1975. Exploration geochemistry distribution of elements and recognition of anomalies. Math. Geol. 7 (5–6), 415–446.
Grigorian, S.V., 1985. Secondary Lithochemical Haloes in Prospecting for Hidden Mineralization. Nedra Publishing House, Moscow (in Russian).
Grigorian, S.V., Ziaii, M., 1997. Computing methods for determination of geochemical haloes background. In: International Symposium, Applied Geochemistry in CIS. IMGRE, Moscow (in Russian).
Harraz, H.Z., Hamdy, M.M., 2015. Zonation of primary haloes of Atud auriferous quartz vein deposit, Central Eastern Desert of Egypt: a potential exploration model targeting for hidden mesothermal gold deposits. J. Afr. Earth Sci. 101, 1–18.
Ke, G., Ling, Ch., Juxing, T., Yanlie, W.U., 2007. The exploring of geochemical concentration focus by fractal content - grads method. Earth Sci. Front. 14 (5), 285–289 (in Chinese).
Levinson, A.A., 1980. Introduction to Exploration Geochemistry. Applied Publishing Ltd., Wilmette, USA (924 pp).
Li, C., Ma, T., Shi, J., 2003. Application of a fractal method relating concentrations and distances for separation of geochemical anomalies from background. J. Geochem. Explor. 77 (2–3), 167–175.
Matveev, A.A., Solovov, A.P., 2011. Geochemical Methods of Exploration of Ore Deposits. Moscow State University, Moscow (in Russian).
Mohammadi, A., Khakzad, A., RashidnejadOmran, N., Mahvi, M.R., Moarefvand, P., Afzal, P., 2013. Application of number–size (N-S) fractal model for separation of mineralized zones in Dareh-Ashki gold deposit, Muteh Complex, Central Iran. Arab. J. Geosci. 6 (11), 4387–4398.
Ovchinnikov, L.N., Grigoryan, S.V., 1978. Geochemical prospecting for ore deposits. Int. Geol. Rev. 20 (12), 1413–1425.
Safari, S., 2017. Geochemical Modeling to Distinguish Zone Dispersed Mineralization (ZDM) from Economic Blind Mineralization (BM) in Urumieh-Dokhtar Arc. Thesis (PhD). Shahrood University of Technology, Faculty of Mining, Petroleum and Geophysics (In Persian).
Safari, S., Ziaii, M., Ghoorchi, M., 2016. Integration of singularity and zonality methods for prospectivity map of blind mineralization. Univ. Tehran Fac. Eng. 50, 189–194.
Safari, S., Ziaii, M., Ghoorchi, M., Sadeghi, M., 2017. Application of concentration gradient coefficients in mining geochemistry: a comparison of copper mineralization in Iran and Canada. J. Min. Environ. 9 (1), 277–292.
Sochevanov, N.N., 1961. Method of sampling of underground workings and surface in search of ore bodies and deposits on the primary dispersion halos. B. Sat: problems. In: Techniques for Testing of Ore Deposits in the Exploration and Exploitation. Gosgeoltekhizdat (in Russian).
Solovov, A.P., 1987. Geochemical Prospecting for Mineral Deposits. Mir, Moscow (in Russian).
Solovov, A.P., Matveev, A.A., 1985. Geochemical Methods of Exploration of Ore Deposits. Moscow State University, Moscow (in Russian).
Soltani, F., Afzal, P., Asghari, O., 2014. Delineation of alteration zones based on Sequential Gaussian Simulation and concentration-volume fractal modeling in the hypogene zone of Sungun copper deposit, NW Iran. J. Geochem. Explor. 140, 64–76.
Timkin, T.V., Lavrov, D.S., Askanakova, O.Y., Korotchenko, T.V., 2014. Structure-geochemical zoning of Topolninsk gold-ore field (Gorny Altai). IOP Conf. Ser. Earth Environ. Sci. 21, 12010.
Valeh, N., 1972. Geological Map of Iran Sheet 7647–Jebal-Barez, scale 1:100,000. Geological Survey of Iran, Tehran.
Vorobiev, S.A., 2016. Informatics, Mathematical Processing of Geological, Geochemical and Ecological Data. Noviyformat (in Russian. 266pp).
Zhou, Y., Ni, S., Shi, Z., 2012. Fractal gradient method to determine the geochemistry anomaly concentration zoning, in Remote Sensing, Environment and Transportation Engineering (RSETE). In: 2012 2nd International Conference on (pp. 1–4). IEEE.
Ziaii, M., 2008. The application of concentration gradient of zonality coefficient for indicator elements as a criterion in mining geochemistry. Goldschmidt Abstracts 2008-Z, 2008. Geochim. Cosmochim. Acta 72, A1105.
Ziaii, M., Pouyan, A.A., Ziaei, M., 2009. Neuro-fuzzy modelling in mining geochemistry: Identification of geochemical anomalies. J. Geochem. Explor. 100 (1), 25–36.
Ziaii, M., Carranza, E.J.M., Ziaei, M., 2011. Application of geochemical zonality coefficients in mineral prospectivity mapping. Comput. Geosci. 37 (12), 1935–1945.
Zuo, R., Xia, Q., Zhang, D., 2013. A comparison study of the C–A and S–A models with singularity analysis to identify geochemical anomalies in covered areas. Appl. Geochem. 33, 165–172.